A COMP DOWNLINK TRANSMISSION SYSTEM VERIFIED BY CELLULAR FIELD TRIALS

Jörg Holfeld, Ines Riedel and Gerhard Fettweis

Vodafone Chair Mobile Communications Systems,
Technische Universität Dresden, 01062 Dresden, Germany
Email: {joerg.holfeld; ines.riedel; fettweis}@ifn.et.tu-dresden.de

ABSTRACT

It is well known in theory that a coordinated multi-point downlink transmission can lead to a significant increase in spectral efficiency for cell-edge users, if channel state information at the transmitter is available. A closed-loop system in conjunction with measurement results of a cellular test bed is presented to conduct a performance comparison between cooperative and non-cooperative base stations.

Since exhaustive field trials with various spatial configurations are very time-consuming, closed-loop real-time measurements were performed on selected positions. The achieved results verify that the observed spectral efficiencies agree with simulative performance predictions based on characterizations of the physical environment. This methodology has been utilized to anticipate the performance in the entire cell area by more feasible field trials.

The achieved cooperation gains are weighted by the geometry factor proportions to draw the comparison with conventional cellular systems.

1. INTRODUCTION

In the recent years, the 3rd Generation Partnership Project (3GPP) Long Term Evolution (LTE) Release 8 standard has been passed and enters the market with commercial products, [1]. The basic concept that is followed in the downlink (DL) embodies the single user (SU) multiple-input multiple-output (MIMO) transmission with orthogonal frequency division multiple access (OFDMA) as modulation and channel access scheme. In cellular communications, such a system comes with the drawback that a frequency reuse planning is compulsory to avoid the multi-user (MU) interference. If the scarce frequency resources cannot be assigned with a reuse factor of one, a loss in terms of the spectral efficiency results. It is well known in theory that a coordinated multi-point (CoMP) DL transmission can lead to a significant increase in the spectral efficiency for cell-edge users, if channel state information (CSI) at the transmitter is available, [2, 3]. These concepts are reflected in the subsequent LTE releases.

The 3GPP consortium pushed the extension of LTE to meet the requirement of a higher demand for cellular broadband communications and quality of service within the entire cell areas. With the coordinated scheduling in Release 9, neighboring base stations (BSs) form a cluster of cells and assign the MU transmission resources jointly for interference avoidance, [4]. With Release 10, namely Long Term Evolution – Advanced (LTE-A), MU interference mitigation can be performed through CoMP by joint transmission (JT). This comprises pre-processing of the DL signals by spatial interference suppressing for non-cooperating mobile terminals (MTs) on the same time-frequency resources.

This contribution presents a prototype CoMP DL system which pre-processes the user data by linear pre-equalization. The resulting spectral efficiencies are measured in a cellular test bed in two typical urban areas. As the conventional reference case, the MTs are served by non-cooperating BSs.

The effort to characterize such a closed-loop system in a cellular environment is tremendously high. Therefore, an evaluation approach will be presented that verifies the closed-loop procedure on selected positions with predicted results from measured channel transfer functions (CTFs). With this method, test bed results are anticipated from CTFs of the entire area. The CoMP performance gains are weighted by the geometry factor proportions of the entire cluster to draw a comparison to conventional cellular systems.

The transmission concept presented in Section 2 motivates the system model given in Section 3. The processing at the BS side is based on estimated CTFs which is a fundamental difference from the assumption of perfectly known CSI at the transmitter (CSIT). The imperfect CSIT leads to an additional error term which is derived in Section 4. Then, closed-loop measurements verify estimated precoding results in Section 5 under the consideration of the error model. Finally, the spectral efficiency gains are discussed in Section 6 to conclude this contribution.

2. BASE STATION AND TERMINAL SIGNAL PROCESSING

This section focuses on the fundamental differences and extensions of the CoMP DL system compared to a conventional LTE Rel. 8 transceiver architecture. The modified processing entities comprise the linear precoder, a modified reference symbol (RS) mapping, the extended feedback to enable the CSIT and the inter BS synchronization. A detailed description of the implemented precoder and the entire system can be found in [5] and [6].

The coarse grain LTE precoder has been replaced by a Wiener transmit filter (TxWF) to mitigate the inter-stream and MU interference among the non-cooperative MTs. The filter coefficients are computed redundantly at each BS from global CSIT by an order-recursive implementation. This algorithm comes with the advantage that a multitude of spatial configurations can be realized as presented in Section 6. Then, each BS selects distinct coefficients to realize the JT. Finally, the precoding filters map the data streams onto the transmit antennas. The transmit filter and the physical MIMO channels form an effective channel by which the received data is observed at the MTs.

Both of the aforementioned channel types must be estimated. Therefore, the DL frame structure has been modified in terms of time-frequency orthogonal RSs. The physical

channel between a transmit and receive antenna pair has to be estimated through the CSI reference symbols (CSI-RSs). The estimates for the allocated frequency resources, the so called physical resource blocks (PRBs), are fed back to the BSs. This provides the CSIT and furthermore the precoding with channel coefficients instead of LTE codebook entries.

In addition to the user data, demodulation reference symbols (DM-RSs) are also passing the precoding block to allow estimates of the effective channel for the data equalization at the MT. The DM-RSs are multiplexed for each stream individually into the transmit data streams after the encoding and modulation have been applied.

The CoMP BSs, which are grouped in a cell cluster, are synchronized by global positioning system (GPS). A common reference clock signal is compulsory to guarantee synchronized local oscillators and a proper sampling. Furthermore, the correct frame timing can be derived. Within this cluster, one BS is selected as serving BS that solely provides the control information of the MTs with the physical downlink control channel (PDCCH). Figure 1 emphasizes the signal processing steps at the BSs. Details about the sensitivity towards timing and frequency errors can be found in [7, 8].

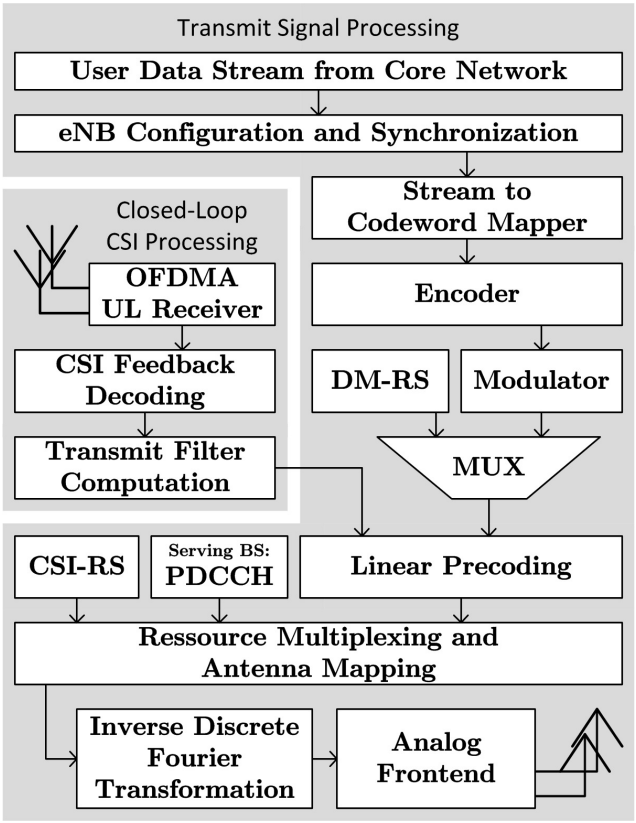

Figure 1: Base station side signal processing steps.

On the MT DL receiver side, similar signal processing steps as in LTE have been realized allowing for the modified subframe structure. The major extension of the system is the compulsory data container for the quantized physical channel coefficients with 8 bit per complex dimension and 3072 bits in total per MT, [6]. The channel feedback is transmitted by each MT via the conventional physical uplink shared channel (PUSCH) on different physical resource blocks (PRBs). In comparison to the non-cooperative LTE Rel. 8 feedback, a few precoding matrix indicator (PMI) bits per subframe and per MT are increased exponentially to roughly 3 Mbit/s/MT, [10]. Indeed, this high rate uplink (UL) feedback is also the major drawback. It limits the spectral efficiency in the UL for the cost of a high CSI resolution at the BS side.

The CSIT is sent back every subframe at a rate of 1 ms as broadcast message to all BSs within the cluster. All BSs decode the PUSCH of every MT individually. Since, there is no additional CSIT synchronization between the CoMP BSs, equal channel knowledge among the transmitters cannot be guaranteed. In contrast to [9], the inter-BS data exchange on the X2 backhaul interface can be avoided.

The closed-loop discussion completes back on the BS side. Here, the channel matrices are multiplexed and forwarded as global CSIT to the precoder. Finally, the transmit filters are applied on the corresponding set of allocated PRBs.

3. SYSTEM MODEL AND SPATIAL SETUPS

The considered CoMP DL scheme comprises spatially distributed BSs with the total number of N_T transmit antennas that serve non-cooperative MTs with the total number of N_R receive antennas. For simplicity, the system model is restricted to a narrow-band system in the spatial domain as

$$\underline{y} = \beta \mathbf{H}\mathbf{W}\underline{x} + \underline{n} \tag{1}$$

with the transmit and receive data symbols $\underline{x}, \underline{y} \in \mathbb{C}^{N_\mathrm{R}\times 1}$, the linear TxWF $\mathbf{W} \in \mathbb{C}^{N_\mathrm{T}\times N_\mathrm{R}}$, the physical channel $\mathbf{H} \in \mathbb{C}^{N_\mathrm{R}\times N_\mathrm{T}}$ and the spatial noise $\underline{n} \in \mathbb{C}^{N_\mathrm{R}\times 1}$. The transmit symbols are modulated and scaled to unit power and the spatial noise is assumed as uncorrelated with the power $\sigma^2_{n_i}$ per i-th receive antenna. In theory [11], the scalar β comprises the sum power constraint. In this implementation, β is used to scale the antenna symbols into the appropriate number representation of the signal processing devices. The system's transmit power is set by the power amplifiers as part of the analog frontend.

The physical channel matrix can be decomposed into

$$\mathbf{H} = \left[\, \underline{h}_1 \quad \dots \quad \underline{h}_{N_\mathrm{R}} \,\right]^T = \begin{bmatrix} \mathbf{H}_{1,1} & \mathbf{H}_{1,2} \\ \mathbf{H}_{2,1} & \mathbf{H}_{2,2} \end{bmatrix}, \tag{2}$$

where the first term contains row vectors that are multiplied by the precoding vectors of the i-th stream and the second term decomposes $\mathbf{H}$ into the local CSIT as used in Section 6. The received symbol at the MT antenna i is given by

$$\underline{y}_i = \underline{h}_i^T \underline{w}_i \, x_i + \sum_{j=1, j\neq i}^{N_\mathrm{R}} \underline{h}_i^T \underline{w}_j \, x_i + \beta^{-1} n_j \;,\; i = 1 \dots N_\mathrm{R} \tag{3}$$

to define the signal-to-interference-and-noise ratio (SINR) as

$$\mathrm{SINR}_i = \frac{|\underline{h}_i^T \underline{w}_i|^2}{\sum_{j=1, j\neq i}^{N_\mathrm{R}} |\underline{h}_i^T \underline{w}_j|^2 + \beta^{-2} \cdot \sigma^2_{n_i}} \tag{4}$$

which expresses the ratio between the desired receive symbol i to the intra- and inter-user interference plus the noise power. This quantity can be directly estimated from the time-frequency orthogonal DM-RS.

Based on the SINR, a theoretical upper bound for a coded transmission is defined by the spectral efficiency [bit/s/Hz]

per stream over $N_{SC} = 120$ sub-carriers of 10 PRBs and 9 OFDM symbols with user data. This results in a block size of $N_{RE} = 1080$ resource elements. Hence, the spectral efficiency is defined with

$$\frac{C(\mathrm{SINR}_i)}{B} = \frac{N_{RE} \cdot \log_2(1+\mathrm{SINR}_i) \;/\; (1\ \mathrm{ms})}{N_{SC} \cdot \Delta f} \quad (5)$$

including the LTE subcarrier spacing Δf of 15 kHz.

The evaluated transmission setup comprises two BSs with two transmit antennas per BS and two MTs with two receive antennas per MT which are served with up to two data streams per terminal. During the measurements, the total number of transmitted spatial streams has been reduced from a 4×4 down to a 4×2 MU-CoMP setup with one stream per MT to present the trade-off between the spatial capacities and transmit diversity gains.

The conventional non-cooperative BS setup has been achieved by nulling the feedback information of the local CSIT $\mathbf{H}_{1,2}$ and $\mathbf{H}_{2,1}$ such that the MU interference mitigation cannot be performed among the distributed transmitters.

4. TRANSMIT FILTER PERFORMANCE DEGRADATIONS UNDER IMPERFECT CSIT

The CSIT are estimates from noisy observations of the physical CTFs which are acquired at the MT side by a least-squares channel estimator. With this approach, the signal-to-noise ratio (SNR) of the CTFs cannot be increased. This imperfect CSIT leads to a mismatch between the real and the observed channel coefficients which are used to compute the precoding matrices. Further performance degradations occur in addition to the spatial noise $\underline{n}$. The aforementioned TxWF has been derived under the assumption of perfect channel knowledge.

Before the relation between measured closed-loop performances and simulative performance estimations can be established in the next section, the error propagation within the precoder must be considered. All field trials are carried out in almost static environments. The recorded CSI was averaged in an off-line evaluation afterwards and the observation noise power could be determined. This procedure motivates to model the imperfect CSI as mean CSI which is perturbed by additive white Gaussian noise (AWGN) with $\widetilde{\mathbf{H}} = \mathbf{H} + \mathbf{E}$ and is uncorrelated between the different antenna links.

Such a CSIT error model has been already discussed in [12]. Here, the mean squared error (MSE) criterion was chosen to express an excess mean squared error (EMSE) in comparison to the achieved minimum mean squared error (MMSE) with the TxWF for the high SNR regime. A simplified EMSE approximation is given in (27) from [12] as

$$\mathrm{EMSE} \approx \mathrm{tr}\left(\left(\mathbf{W}^{*}\mathbf{W}^{T} \otimes \mathbf{H}\mathbf{W}\right)\boldsymbol{\Sigma}\right) \quad (6)$$

with $\mathbf{W}$ as TxWF based on averaged channel coefficients $\mathbf{H}$. The covariance matrix $\boldsymbol{\Sigma} \in \mathbb{C}^{N_T N_R \times N_T N_R}$ contains the individual observation noise covariance between the transmit and receive antenna pairs

$$\boldsymbol{\Sigma} = \mathscr{E}\left\{\mathrm{vec}(\mathbf{E})\mathrm{vec}(\mathbf{E})^{H}\right\}. \quad (7)$$

Since uncorrelated noise is assumed, $\boldsymbol{\Sigma}$ reduces to a diagonal matrix with the elements $[\boldsymbol{\Sigma}]_{ii} = \sigma_{ii}^2$ and $i = 1, \ldots, N_T \cdot N_R$.

In the latter, the EMSE normalized to N_R is used as additional impairment beside the spatial noise and MU interference. Furthermore, it is the used quantity that reduces the bias between measured and estimated SINRs.

5. MEASURED SINR AND PREDICTED SINR

Exhaustive closed-loop measurements with various spatial configurations over the entire cell area are hard to achieve. Therefore, a more sophisticated solution leads to an anticipation of cellular results in large scale. Feasible field trial campaigns can be conducted if the entire signal processing chain is emulated with the bit-true signal representations only based on open-loop physical channel measurements.

With that idea, a twofold field trial campaign has been accomplished: At first, closed-loop real-time measurements were performed on selected positions to verify the estimated SINR based on physical CTFs. The excess error model of the noisy CSI is included into the SINR prediction to reduce the bias of the performance results. Secondly, another field trial followed to record the aforementioned CTFs for a further off-line evaluation. Figure 2 illustrates the positions for two different test bed areas in downtown Dresden, Germany, and for two CoMP BSs on a single site.

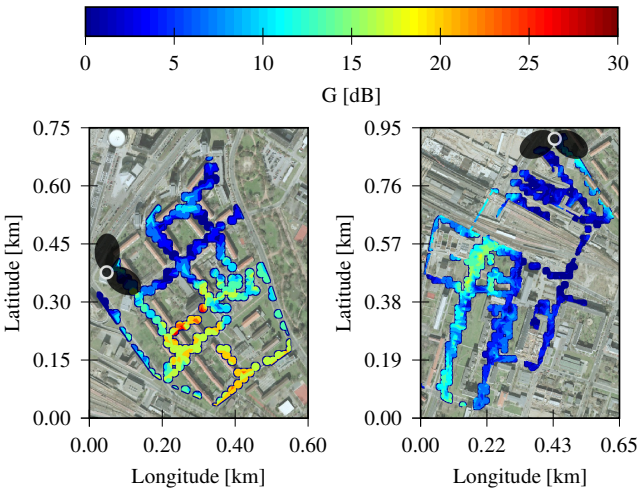

(a) Northern test bed area. (b) Southern test bed area.

Figure 2: Absolute geometry factors [dB] in the field trial area. The maps are provided by the courtesy of Google maps.

Figure 3 shows the mapping of the measured SINR onto the predicted SINR for the CoMP configurations considering the imperfect CSIT. On average, the SINRs are underestimated below 5 dB while an overestimation for values above 10 dB occurs.

6. TESTBED RESULTS

The geometry factor (GF) is used to quantify the mean receive power level of the serving BS to the mean interference level from the second BS over N CSI-RS observations with the second term of (2)

$$\mathrm{G} = \left| 10 \cdot \log_{10}\left(\frac{\sum_{n=1}^{N}(\,\mathbf{H}_{1,1}[n]\,)^2}{\sum_{n=1}^{N}(\,\mathbf{H}_{1,2}[n]\,)^2} \right) \right|. \quad (8)$$

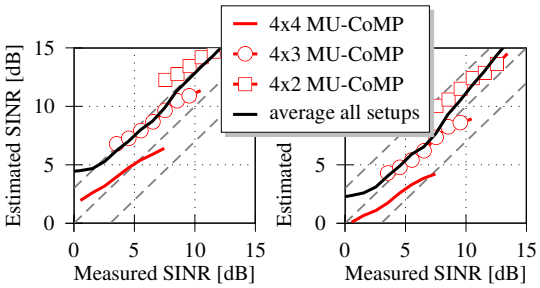

(a) Without EMSE. (b) With EMSE.

Figure 3: SINR mapping function.

Based on the GF, places with symmetric and asymmetric receive power levels can be indicated as cell-edge and cell-center. Figure 2(a) highlights some positions with equal power ratios of 0 dB for the northern test bed area. Here, shadowing through prominent buildings causes a diverse behavior and results in a narrow cell-edge area. The southern area in Figure 2(b) shows a much wider cell-edge with only a few shadowing effects. In both figures the measured cell-edge agrees with the geometric cell-edge of the spanned sectors. More details of the considered area with additional propagation timing metrics can be found in [6].

Two MTs are classified according to their geometry factors from the set of measured CSITs. The first one is assigned to the first BS as serving BS and the second is the interfering one. For the second MT, the BS assignment is performed in the opposite way. Finally, the two MTs are grouped for a CoMP DL transmission if their geometry factors are equally classified with respect to the different serving BSs. This criterion allows a separation of cell-edge and cell-center results.

Figure 4(a) and Figure 5(a) review two results from [6] and depict the sum over the anticipated spectral efficiencies per stream as a function of the symmetric geometry factors for the different spatial configurations. In the northern area, the increase in the sum spectral efficiency with additional spatial streams reflects the rich scatting environment. In contrast to that, the south does not provide significant transmit diversity gains due to the dominant line-of-sight (LOS). A trade-off between the number of spatial streams and worse interference mitigation is observed. In particular, the performance gains of the BS cooperation can be seen at the cell-edge with 138% (north) and 116% (south). The spectral efficiency converges to the results of the conventional transmission if the MT are position closed to their cell-centers.

In contrast to [6], the CoMP DL gain in Figure 4(c) must be evaluated under the distribution of the cell-edge area compared to the size of the entire cell-cluster. The plotted histogram of the GF in Figure 4(b) agrees with the narrow cell-edge and the faster convergence of spectral efficiencies towards the cooperative transmission. If the spectral efficiencies conditioned on the geometry factors are weighted by their distributions then an overall performance gain of 31.6% is determined between the 4×4 MU-CoMP and the conventional case. The gain in the southern area (see Figure 5(c)) is caused by the wider relative cell-edge area in this cluster (see Figure 5(b)) and results in 55.5% of improvement.

Finally, another result must be emphasized, too. BS cooperation in the downlink achieves fairness over the entire cluster area. Here, a more homogeneous SINR distribution can be realized. This behavior is reflected in Figures 4(d) and 5(d) by the standard deviations of the sum spectral efficiencies. The non-cooperative transmission results in a much higher spreading of the observed spectral efficiency.

7. SUMMARY AND OUTLOOK

With this contribution, a CoMP DL real-time system was introduced with the focus on the basic extensions from the 3GPP-LTE release 8. Before field trial results are presented, the system model under imperfect CSIT was discussed. From the field trials, a spectral efficiency gain by BS cooperation at the cell-edges of at least 100% could be observed. If these results are related to the entire cell area then the performance gains reduce significantly depending on the relative cell-edge size. However, the BS cooperation significantly improves the fairness over the entire cluster area.

Motivated by [13] and considering that the gains achieved in the test bed are based on the cooperation of co-located BSs, future measurements could include the investigation of the impact of the extent of sectorization and the antenna directivity.

Some important issues to determine the gains of CoMP in a fair comparison to non-cooperative BSs are not addressed here. In a next step, scheduling must be in-cooperated. A certain set of users may be assigned to orthogonal transmission resources before a certain amount of traffic load requires running the entire cellular system with a frequency reuse of one. Additionally, other results show tremendously performance losses if such kind of linear filter is reused with a much higher quantization as used here. Also the feedback update rate should be adapted according to the coherence time of the physical environment.

Only if the mentioned impairments can be handled with robust technical solutions then a commercial roll-out of such a base station cooperation scheme in the downlink is feasible.

REFERENCES

[1] 3GPP Technical Specification 36.213 v8.8.0, "Evolved Universal Terrestrial Radio Access (E-UTRA); Physical layer procedures (Release 8)," September 2009.

[2] D. Gesbert, S. Hanly, H. Huang, S. Shamai Shitz, O. Simeone, and Wei Yu, "Multi-Cell MIMO Cooperative Networks: A New Look at Interference," *Selected Areas in Communications, IEEE Journal on*, vol. 28, no. 9, pp. 1380 –1408, december 2010.

[3] R. Irmer, H.-p. Mayer, A. Weber, V. Braun, M. Schmidt, M. Ohm, N. Ahr, A. Zoch, C. Jandura, P. Marsch, and G. Fettweis, "Multisite field trial for LTE and advanced concepts," *Communications Magazine, IEEE*, vol. 47, no. 2, pp. 92 –98, february 2009.

[4] 3GPP Technical Report 36.814 v9.0.0, "Further Advancements of E-UTRA Ű Physical Layer Aspects (Release 9)," March 2010.

[5] J. Holfeld, V. Kotzsch, and G. Fettweis, "Order-Recursive Precoding for Cooperative Multi-Point Transmission," in *Proc. Int Smart Antennas (WSA) ITG Workshop*, 2010, pp. 39–45.

[6] J. Holfeld, E. Fischer, and G. Fettweis, "Field Trial Results for CoMP Downlink Transmissions in Cellu-

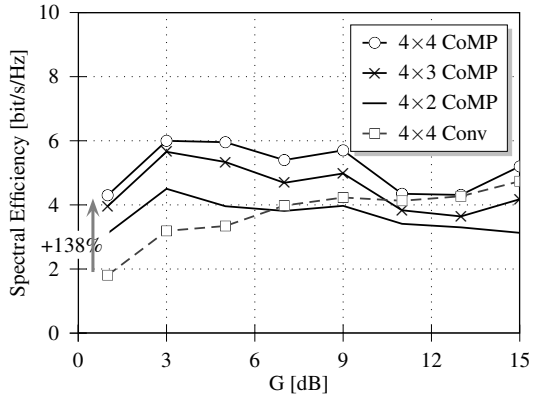

(a) The average spectral efficiencies of all transmitted streams as function of the geometry factors.

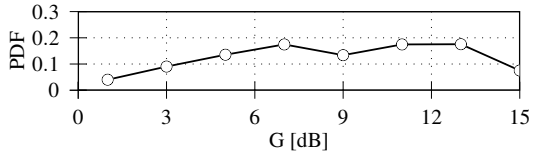

(b) The probabilities of the observed geometry factors.

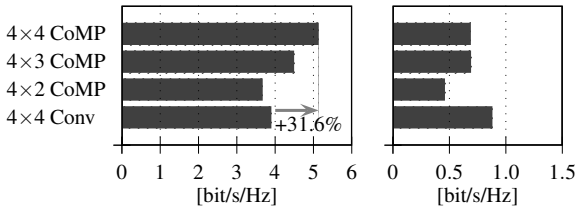

(c) Area weighted spectral efficiencies.

(d) The standard deviation.

Figure 4: Spectral efficiencies in the northern test bed area.

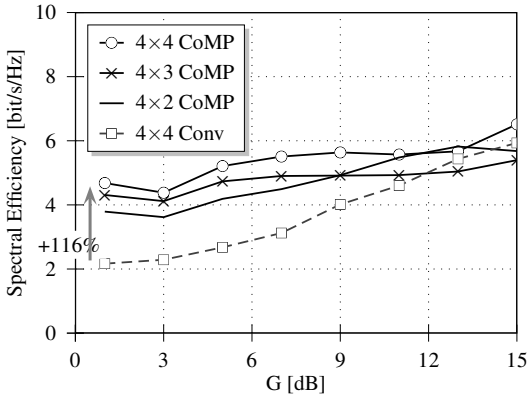

(a) The average spectral efficiencies of all transmitted streams as function of the geometry factors.

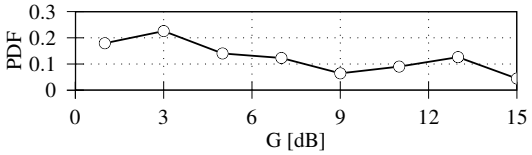

(b) The probabilities of the observed geometry factors.

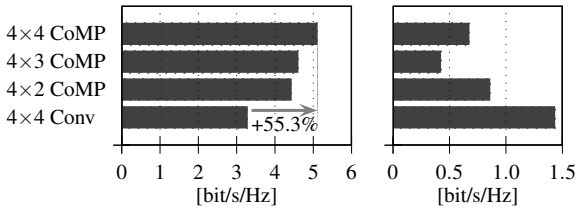

(c) Area weighted spectral efficiencies.

(d) The standard deviation.

Figure 5: Spectral efficiencies in the southern test bed area.

lar Systems," in *Proc. Int Smart Antennas (WSA) ITG Workshop*, 2011, pp. 1–7.

[7] M. Morelli, C.-C.J. Kuo, and M.-O. Pun, "Synchronization Techniques for Orthogonal Frequency Division Multiple Access (OFDMA): A Tutorial Review," *Proceedings of the IEEE*, vol. 95, no. 7, pp. 1394 – 1427, july 2007.

[8] V. Kotzsch, J. Holfeld, and G. Fettweis, "Joint Detection and CFO Compensation in Asynchronous Multi-User MIMO OFDM Systems," in *Proc. IEEE 69th Vehicular Technology Conf. VTC Spring 2009*, 2009, pp. 1–5.

[9] V. Jungnickel, L. Thiele, T. Wirth, T. Haustein, S. Schiffermuller, A. Forck, S. Wahls, S. Jaeckel, S. Schubert, H. Gabler, C. Juchems, F. Luhn, R. Zavrtak, H. Droste, G. Kadel, W. Kreher, J. Mueller, W. Stoermer, and G. Wannemacher, "Coordinated Multipoint Trials in the Downlink," in *Proc. IEEE GLOBECOM Workshops*, 2009, pp. 1–7.

[10] Farooq Khan, *LTE for 4G Mobile Broadband: Air Interface Technologies and Performance*, Cambridge University Press, New York, USA, 2009.

[11] M. Joham, W. Utschick, and J.A. Nossek, "Linear transmit processing in MIMO communications systems," *Signal Processing, IEEE Transactions on*, vol. 53, no. 8, pp. 2700 – 2712, august 2005.

[12] D. Tsipouridou and A.P. Liavas, "On the Sensitivity of the Transmit MIMO Wiener Filter With Respect to Channel and Noise Second-Order Statistics Uncertainties," *Signal Processing, IEEE Transactions on*, vol. 56, no. 2, pp. 832 –838, feb. 2008.

[13] I. Riedel, P. Rost, P. Marsch, and G. Fettweis, "Creating Desirable Interference by Optimized Sectorization in Cellular Systems," in *Proc. IEEE Global Telecommunications Conf. GLOBECOM 2010*, 2010, pp. 1–5.